# INTERFEROMETRY WITH X RAYS

Interference patterns of diffracted x rays are so sensitive to small displacements that we can see strains and defects in crystals. Interest now is in absolute measurements of lattice spacings and fundamental constants.

# Michael Hart and Ulrich Bonse

In this new branch of applied x-ray optics, crystals that obey Bragg's law of reflection are used as optical components. The physics of these devices is very simple and has long been available in the works of, for example, Max von Laue and Paul Ewald. Construction and operation of x-ray interferometers, however, had to await the arrival of large, almost perfect, artificially grown single crystals. In the five years that have elapsed since the first successful x-ray interferometer was made<sup>1,2</sup> only a few of the possible applications have been exploited.

What makes x-ray interferometry such a useful technique? For x rays the refractive index n of all materials is just less than unity, about  $1 - 10^{-5}$ . This situation makes conventional specular reflection techniques unfeasible-the critical angle is very small (about 1/2 deg), and the focal length of lenses would be at least a few kilometers. In contrast to the disadvantages for conventional optical techniques are the advantages for interferometry, where the need is to balance optical path lengths; the physical dimensions need only be accurate to  $[1/(1-n)] \lambda = 10^5 \lambda$ , a length of the order of tens of microns.

Perfect crystals Bragg-reflect x rays only over a very narrow range of incident angles, about 10<sup>-5</sup> radians. The degree of lattice perfection is, therefore, very important in determining the relative phases of the beams that

an x-ray interferometer generates. This sensitivity allows one to measure phase shifts resulting from strains in the diffracting crystals as well as shifts caused by objects placed in the path of an interferometer beam. X-ray interferometers are used to make absolute measurements of lattice spacings, to compare these spacings, to characterize defects in good single crystals, to measure x-ray scattering factors and to do x-ray phase-contrast microscopy. Existing x-ray interferometers use both Bragg-case diffraction, in which the beam enters and exits from the same surface of the crystal, and Laue-case diffraction, in which the entrance and exit beams are at different surfaces. All applications to date, however, have been with Laue-case diffraction.

## Diffraction in crystals

We formulate the general problem of x-ray diffraction by perfect crystals before we can discuss the special cases that are used in interferometers. We use a periodic complex dielectric constant to describe the crystal and then find the allowed waves. These are the waves that satisfy Maxwell's equations as well as the Laue equation

$$\mathbf{K}_{o} + \mathbf{h} = \mathbf{K}_{h} \tag{1}$$

Here  $\mathbf{K}_o$  and  $\mathbf{K}_h$  are the wave vectors for the incident and diffracted waves, and  $\mathbf{h}$  is the reciprocal lattice vector for the acting Bragg reflection ( $|\mathbf{K}_o|$  =  $|\mathbf{K}_h|$ ;  $|\mathbf{h}|^{-1} = d$ , the Bragg spacing).

In most cases, it is not really useful to think of two separate waves, the incident and the diffracted, inside the crystal, but the separation helps in the general formulation. When considering specific cases, we think instead of the total wavefield inside the crystal.

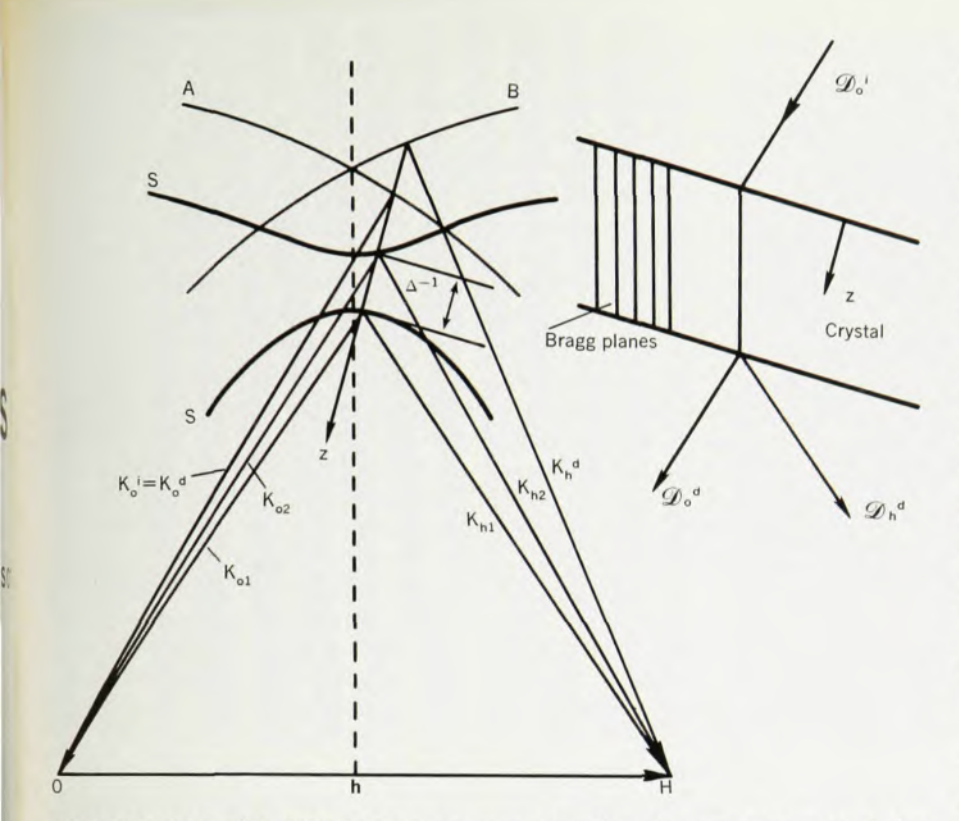
At angles close to the exact Bragg-reflection position, both wave vectors end near the Brillouin-zone boundary. We expect, from Maxwell's equations, two solutions for each state of polarization, and indeed we find waves with wave vectors  $\mathbf{K}_{h1}$ ,  $\mathbf{K}_{o1}$ ,  $\mathbf{K}_{h2}$ ,  $\mathbf{K}_{o2}$  and amplitudes  $D_{h1}$ ,  $D_{o1}$ ,  $D_{h2}$ ,  $D_{o2}$  such that

$$\mathbf{K}_{h1} - \mathbf{K}_{o1} = \mathbf{K}_{h2} - \mathbf{K}_{o2} = \mathbf{h}$$
 (2)

That is, the wave is split close to the Brillouin zone (analogous to the behavior of electron waves in band conductors) into two complementary waves, each of which satisfies the Laue equation. In any real case the incident wave, with time-dependent amplitude  $\mathfrak{D}_{o}^{\ i} = D_{o}^{\ i}$  exp  $[2\pi i(v\tau - \mathbf{K}_{o}^{\ i} \cdot \mathbf{r})]$  excites only certain wavefields in the crystal; allowed waves are constrained by Snell's law

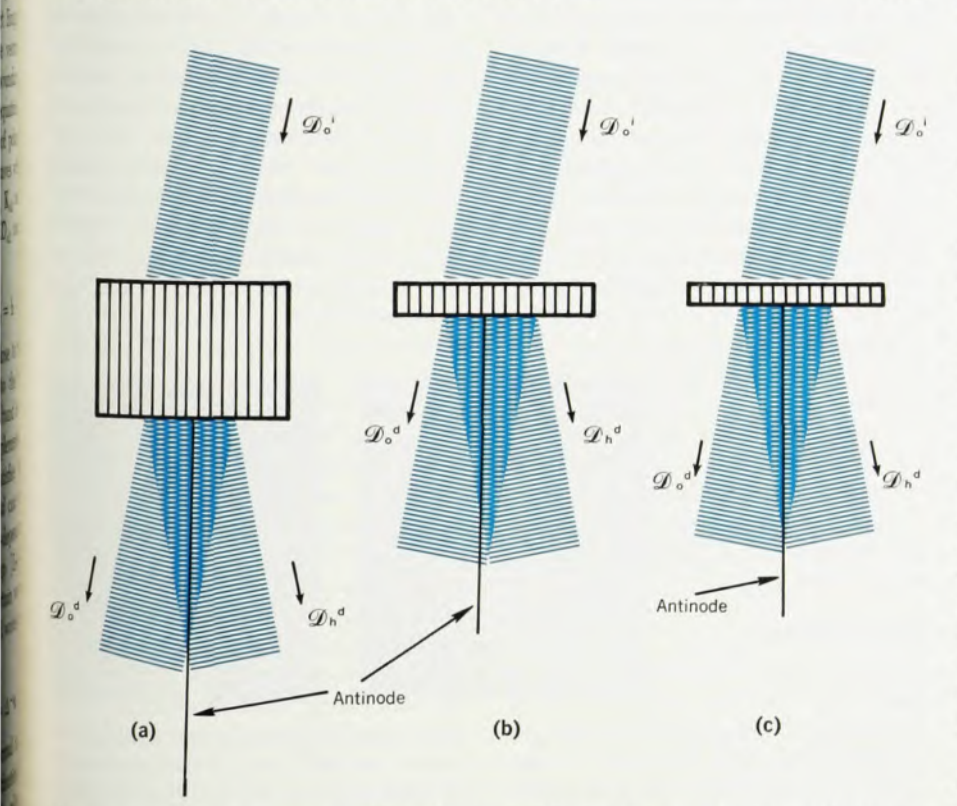
$$\mathbf{K}_{h2} - \mathbf{K}_{h1} = \mathbf{K}_{o1} - \mathbf{K}_{o2} = \Delta^{-1}\mathbf{z}$$
 (3)

Here z is a unit vector normal to the crystal surface, and the extinction distance  $\Delta^{-1}$  is a measure of the splitting, as shown in figure 1.  $\Delta$  is proportional to the strength of the interaction in the crystal, but varies with the angle of incidence and is of the order of



GEOMETRICAL RELATIONSHIPS between the allowed wave vectors K during Bragg reflection. A and B are spheres of radius  $1/\lambda$  and are centered, respectively, at the origin O and reciprocal lattice point H. The dispersion surface S is the locus of tips of the allowed wave vectors in the diffracting crystal, and the normal, z, ties these vectors to the incident wave vector  $K_0^{-1}$ . Note that  $\Delta$ , the extinction distance, is a function of the orientation of both  $K_0^{-1}$  and z. Subscript o refers to incident wave and h to diffracted wave in the crystal, i and d are incident and diffracted waves outside the crystal, and 1 and 2 are the two components into which each wave is split as it approaches the region close to the Brillouin zone.

—FIG. 1



ANTINODES OF THE STANDING WAVEFIELD lie halfway between the atomic planes (vertical lines) for the thick crystal case (a). For the thin crystal case, we may choose the thickness so that the antinodes will lie either d/4 to the right (b) or d/4 to the left (c) of the atomic planes in the crystal.

 $(1-n)\lambda^{-1}$ . We need not carry out a detailed solution of Maxwell's equations here but will instead consider several special cases to understand how the various diffracting elements in an x-ray interferometer work.

#### Special cases

Consider a simple crystal structure in which all of the atoms lie on the family of planes  $\mathbf{r} \cdot \mathbf{h} = p$ , where p is an integer. If the crystal is thick enough there is only one wavefield present, the wavefield that has nodes at the atomic sites and maximal amplitude halfway between the atomic nuclei. The other, complementary, wavefield is essentially totally attenuated by the innershell electrons near the atomic sites. That is, we find when we solve Maxwell's equations that  $D_{\rm h1}/D_{\rm o1} = \xi_1 \approx 0$  and  $D_{\rm h2}/D_{\rm o2} = \xi_2 < 0$ .

In the first x-ray interferometers, for example, all of the x-ray optical components were silicon crystals approximately 0.5 mm thick. For the 220 Bragg reflection of copper  $K\alpha$  radiation ( $\lambda=0.154$  nanometers) these are effectively opaque to type-1 wavefields (the wavefields with antinodes at the atomic nuclei). At this wavelength almost all of the photoelectric absorption in silicon is associated with the K-shell electrons.

The total wavefield has intensity

$$|D_2|^2 = |D_{h2} + D_{o2}|^2 \propto 1 + \xi_2^2 + 2\xi_2 \cos(2\pi \mathbf{h} \cdot \mathbf{r})$$
 (4)

 $\xi_2$  varies with the angle of incidence of the primary wave.

We see then that wavefield 2 survives because it suffers less than normal photoelectric attenuation. This "anomalous transmission" effect is well known in good single crystals and was first discovered by Gerhardt Borrmann.<sup>7</sup>

Outside the crystal we again form two diffracted waves of amplitudes  $\mathfrak{D}_{\,\mathrm{o}}{}^{\mathrm{d}}$  and  $\mathfrak{D}_{\,\mathrm{h}}{}^{\mathrm{d}}$  (see figure 2a). Together they make up the wavefield of equation 4 inside the crystal and in their overlap region. The crystal lattice "phase locks" them to each other; the crystal is a phase-coherent beam splitter and a phase-maintaining mirror that bends rays through twice the Bragg angle.

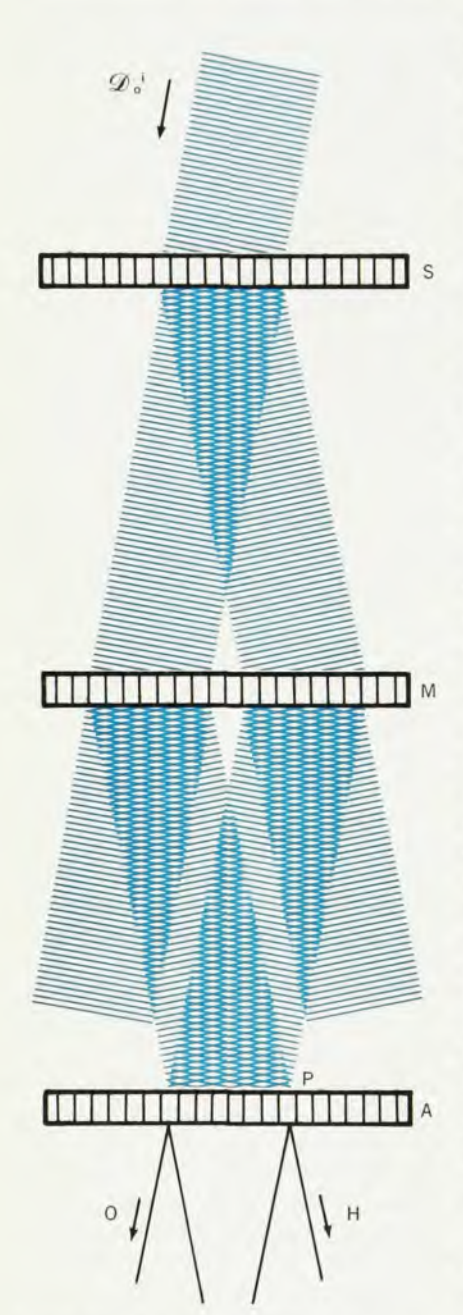
For the other extreme, the thincrystal case, all four waves are present and  $D_{\rm h1}/D_{\rm o1}=\xi_1>0$ ,  $D_{\rm h2}/D_{\rm o2}=\xi_2<0$ . At the exact center of the range, for the symmetric Laue case,  $\xi_2=-\xi_1$ . Wavefield 2 again has the intensity given by equation 4 and wavefield 1 has complementary intensity

$$|D_1|^2 = |D_{h1} + D_{o1}|^2 \propto 1 + \xi_1^2 + 2\xi_1 \cos(2\pi \mathbf{h} \cdot \mathbf{r})$$
 (5)

All of the fields generated are phase coherent, and the total field is

$$|D|^2 = |D_{h1} + D_{o1} + D_{h2} + D_{o2}|^2 \propto$$
  
  $2 + 2 \sin(2\pi \mathbf{h} \cdot \mathbf{r}) \sin(2\pi \Delta^{-1}t)$  (6)  
where  $t$  is the crystal thickness.

Again the crystal is a phase-coherent beam splitter and an optical mirror; outside the crystal we have the



LAUE-CASE interferometers. Phase-coherent beams are formed successively at beam splitter S and transmission mirror M, and culminate in an atomic-scale standing wavefield at point P in front of the analyzing crystal.

—FIG. 3

two diffracted waves  $D_0^d$  and  $D_h^d$  generated from a standing wavefield that fits onto the diffracting planes.

(Although we can not achieve zero absorption conditions, we do have interferometers with 0.2 mm-thick silicon or quartz wafers that we have operated with molybdenum  $K^{\alpha}$  ( $\lambda = 0.071$  nm) and silver  $K^{\alpha}$  ( $\lambda = 0.056$  nm) radiation. Here the two wavefields do not have exactly equal intensities, but the essential features described by equation 6 are the same.)

The situation here is more complicated than is the first case, because the last term in equation 6 is a periodic function of t. The thickness influences both the amplitude of modulation and the position of the intensity field with respect to the crystal, as can be seen in figures 2b and 2c. By a suitable choice of thickness, we can use the crystal either as an ideal mirror  $[t = p\Delta \text{ or } t = (p + 1/2)\Delta]$ or, with  $t = (p \pm 1/4) \Delta$ , as an ideal beam splitter. In practice we get high intensity because we use a slightly divergent incident beam rather than a plane wave. A disadvantage of the range of incident angles is that the ideal crystal thickness does not have a unique value, but has a range, because of the variation of  $\Delta$ .

In the Bragg case the orientation of the diffracting planes is such that Ko is directed into the crystal whereas Kh points out of the front surface of the crystal. The diffracted wave Dnd comes out at the front surface, and some energy flows into the interior of the crystal to form a standing wavefield. If the crystal is very thin, some energy reaches the rear surface of the crystal plate, where a second diffracted wave Dod is emitted. The two emitted waves are phase coherent, because the standing wavefield inside the crystal couples them. We have made x-ray interferometers with Bragg-case optical components in our laboratory and obtained adequate intensity for photographing fringe patterns by using silicon crystals a few tenths of a millimeter thick.

#### Interferometry

Applied x-ray interferometry has to date used Laue-case diffraction in all of the optical components, because the physical parameters are easier to work with. Figure 3 shows the layout of a Laue-case interferometer that uses thick crystals. In each wafer only one pair of waves is present. The condition that the wavefield-intensity max-

ima must lie between the planes of atoms dictates the phase of the newly generated wave. (See equation 4.)

Had we chosen instead to illustrate the thin-crystal case, we would have had intensity maxima in the standing wavefield outside of each crystal as in figures 2b and 2c, either 1/4 d to the right or 1/4 d to the left of the planes of atoms. In either case, a standing wavefield is formed at P, and the relative phases of the waves arriving along the two paths to P determine the position of these fringes. The analyzer crystal A transforms the atomic-scale fringe pattern at P into a macroscopic pattern that we can observe either on film or with a counter in one of the exit beams. This macroscopic pattern is simply the moiré pattern resulting from the superposition of the atomicscale standing-wave pattern at P with the atomic planes of A. If we introduce inhomogeneous phase shifts into one of the arms of the interferometer. either the orientation or the spacing of the standing wave pattern will be changed. We will then observe either a rotational or a dilational moiré pattern, or a pattern that is a combination of the two.

What happens if we displace the diffracting wafer by a distance c with respect to the x-ray source? The phase of Dod is unchanged, and the phases of the reflected waves Dhd are altered by  $2\pi$  h·c. The relative positions of all parts of an interferometer, therefore, must be maintained so that hec >> 1 or  $|\mathbf{c}| < 10^{-2}$  nm. For this reason most x-ray interferometers made so far have been cut as monolithic blocks from highly perfect crystals. There are, of course, advantages to this extreme sensitivity, and we can exploit it to measure displacements of the order of 10-2 nm.

Placing a phase-shifting object in either of the interfering beam paths causes changes in the position of the standing-wave pattern at P. A lens-shaped object, for example, forms a moiré pattern similar to the well known Newton's-ring pattern in light optics.<sup>8</sup> An object of material thickness between one and 50 microns typically causes a phase advance of  $2\pi$ , and x-ray interferometers have been used to measure material thickness<sup>9</sup> as well as to measure x-ray refractive indices<sup>10,11</sup> and atomic-scattering factors for x rays.

X-ray interferometers have significant advantages for these determinations. Traditional x-ray methods of





TWO DISLOCATIONS IN A SILICON INTERFEROMETER cause rotational moiré pattern (a). Reciprocal lattice vector h is 220, and field is approximately 4.5 mm by 4.0 mm. Copper  $K\alpha$  radiation was used to obtain the pattern. Elastic strains in silicon caused by evaporating four thin aluminum-film discs on to the analyzer crystal can also be seen in a moiré pattern (b). The discs, each of diameter 5 mm, vary in thickness up to 500 nanometers. Molybdenum  $K\alpha_1$  radiation was used to obtain the pattern; here again the reciprocal lattice vector is 220.

—FIG. 4

measuring material thickness for example, are based on absorption, which increases as the fourth power of the atomic number Z. For heavy atoms, the absorption is very high, whereas the method is insensitive for light atoms. Phase advance, on the other hand, increases linearly with Z. To measure n with, say, a prism, we would need a large-angle prism (because  $n \approx 1$ ). Again, absorption

causes difficulties. We have been able to improve the precision in measuring atomic-scattering factors by about an order of magnitude.

No one has as yet exploited x-ray interferometers in phase-contrast microradiography. This technique would be useful in studies of biological materials; sensitivity is retained even in the analysis of light elements, and we can distinguish between car-

bon, nitrogen and oxygen even with material only a few microns thick.

# Lattice parameters

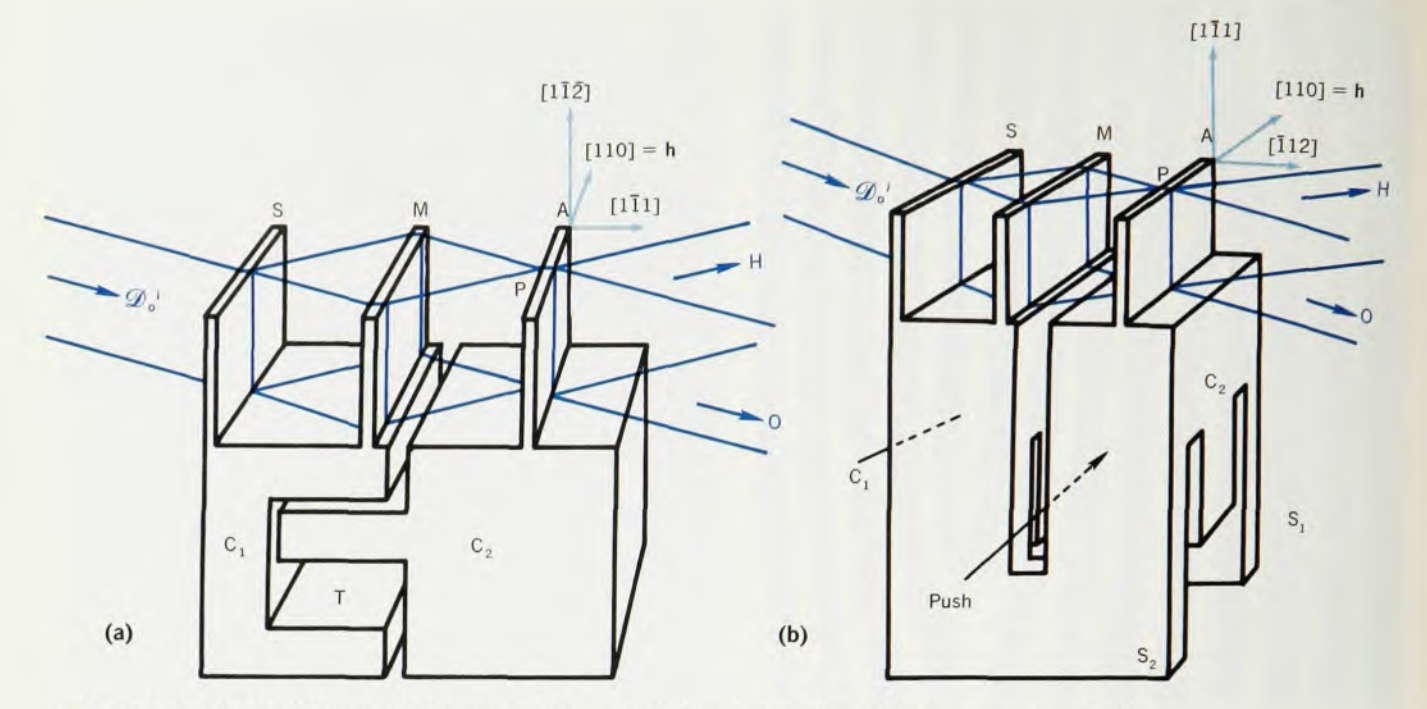
If one or more of the diffracting wafers of an x-ray interferometer is strained, then a moiré pattern is generated in the exit beams O and H. When we strain one wafer homogeneously, so that its reciprocal lattice vector becomes h + 8h, the reciprocal vector of the moiré pattern is 8h. For a small rotation  $\phi$ , we see moiré fringes parallel to h with a spacing  $\Lambda_R = d/\phi$ , whereas a small dilation  $\delta d/d$  produces moiré fringes normal to h with spacing  $\Lambda_{\rm D} = d^2/\delta d$ . Both these simple cases have been demonstrated quantitatively with a Laue-case interferometer.12 Because we can measure fringe spacings up to 2 cm, we can detect lattice rotations  $\phi \approx 10^{-8}$  rad or dilations  $\delta d/d \approx 10^{-8}$ .

Inhomogeneous strain also produces moiré fringe patterns in the exit beams. For example, crystal dislocations in the interferometer wafers cause fringe dislocations in the moiré pattern. Figure 4a is a rotational moiré pattern with  $\phi \approx 0.13$  sec arc, and shows two dislocations of opposite sign in a silicon interferometer. From the known





Michael Hart (left) and Ulrich Bonse will receive the American Crystallographic Association's Warren Award this month for work, described in this article, that the two did together at the Cornell University department of materials science and engineering. Hart, who received his PhD from the University of Bristol in 1963, is presently on leave from his post as lecturer in physics at Bristol; he is a US National Academy of Sciences senior research associate at the NASA electronics research center in Cambridge. Now professor of physics at the University of Münster, Bonse received the Diplomphysiker in 1955 and was awarded a Dr. rer. nat. habil. in 1963.



SCANNING X-RAY INTERFEROMETER. Two-part design (a) is for absolute measurement of lattice parameters. Crystal block C<sub>1</sub> is translated parallel to h on a specially constructed traversing device. Relative orientations of C<sub>1</sub> and C<sub>2</sub> are controlled with multiple Bragg reflections in the tunnel T and through the interferometer wafers S, M and A. Scanning interferometer may also be a monolithic structure (b). A push in the appropriate place translates the analyzer wafer A on block C. This pushing causes elastic deformation of the two bent leaf springs S<sub>1</sub> and S<sub>2</sub>, and translation parallel to h. The silicon crystal is almost perfect, so that it can tolerate large strains without undergoing plastic deformation; a 0.7 mm range has been obtained on a device only 30 mm high. —FIG. 5

value of d and the observed number of extra half fringes, we can measure directly the dislocation (Burgers) vector:  $\mathbf{b} = 1/2 < 110 > = 0.384$  nm. We have observed many other intrinsic strain patterns in silicon, quartz and germanium interferometers,  $^{13}$  and consider we have an extremely sensitive method for detecting and characterizing strains in single crystals.

We have also used moiré mapping of large crystal areas to measure intentionally induced strains in otherwise perfect crystals.<sup>14</sup> In the manufacture of a semiconductor one might diffuse in some impurity locally; moiré mapping can determine how much has been diffused in. If an impurity introduced into a silicon crystal, for example, has a covalent radius 10% different from that of silicon, one part per million of the impurity will change d by one part in  $10^7$ . We can see this strain with moiré mapping.

In figure 4b we see the moiré pattern formed when four aluminum discs of various thicknesses were evaporated onto the analyzer wafer of a thincrystal Laue-case interferometer. Repetitive exposures, with and without the discs present, prove the strains to be purely elastic; they are simply bimetal strains caused by the difference in thermal-expansion coefficients between silicon and aluminum. Maximal strain occurs at the center of the thickest disc where the moiré spacing, 0.2 mm, corresponds to  $\delta d/d=10^{-6}$ .

Perhaps the most important application discovered so far for the Lauecase interferometer is in metrology and fundamental constants. If we displace the analyzer of an interferometer by an amount c, a phase shift of  $2\pi h \cdot c$ in the output beams results. - If we shift the analyzer parallel to h, but with otherwise perfect control of orientation and stability, one moiré fringe will be recorded in the exit beams when ch changes by unity, whatever x-ray wavelength is used. If displacement is simultaneously measured2 with an optical interferometer, we have a way to measure lattice parameters without a measurement of x-ray wavelength. The measurement results in a much needed secondary standard of length equal to the lattice spacing of the analyzer crystal. In addition, measurements of the crystal density and atomic mass permit one to determine Avogadro's number.

If we cut the interferometer into two parts, which are then reassembled on adequately stable goniometric and translation stages, we can make translations of the analyzer crystal. Erich te Kaat and one of us use designs such as the one in figure 5a to measure<sup>15,16</sup> absolute lattice parameters; Richard Deslattes at the US National Bureau of Standards later adopted<sup>17</sup> the design for the same purpose.

In this design, control of the relative orientations of the two separated crystals about the [1 1 1] axis (the rotational moiré axis) is achieved by x-ray beams from an auxiliary source. These beams are multiply Bragg-reflected by the 224 and 224 planes that form the top and bottom walls of the tunnel between the two crystals. The translation stage makes extensive use of elastic design principles.

A group of workers from the University of Bristol and the National Physical Laboratory (UK) have adopted<sup>18,19</sup> a rather different approach. The x-ray interferometer and the elastic springstrip translation stage are all part of the same almost perfect crystal (see figure 5b). Pushing at the appropriate point results in a translation of

the analyzer wafer parallel to h. This system is very stable and, of course, is prealigned. Special miniature optical components are, however, needed in the associated optical interferometer.

At a time when traditional x-ray methods no longer have a significant role in determining the fundamental constants of physics, it is exciting that these new devices should soon produce significant advances in our knowledge of these constants.

Because each component in an x-ray interferometer may use thick or thin Laue-case diffraction or Bragg-case diffraction, and because the interferometer can be cut in one or more parts. there are many possible designs. Some have been put into practice<sup>8,20,21</sup> and others have very interesting and useful characteristics,22 but the vast majority still await exploitation.

#### References

- 1. U. Bonse, M. Hart, Appl. Phys. Lett. 6, 155 (1965).
- 2. U. Bonse, M. Hart, Z. Phys., 188, 154 (1965).
- 3. M. von Laue, Röntgenstrahlinterferenzen, Akademische Verlag, Frankfurt (1960).
- 4. R. W. James, The Optical Principles of the Diffraction of X-rays, Bell, London (1948).
- 5. B. W. Batterman, H. Cole, Rev. Mod. Phys. 36, 681 (1964).
- 6. J. C. Slater, Rev. Mod. Phys. 30, 197 (1958).
- 7. G. Borrmann, Naturwiss. 38, 330 (1951).
- 8. U. Bonse, M. Hart, Appl. Phys. Lett. 7, 238 (1965).
- 9. N. Kato, S. Tanemura, Phys. Rev.
- Lett. 19, 22 (1967). 10. U. Bonse, H. Hellkötter, Z. Physik 223, 345 (1969).
- 11. D. C. Creagh, M. Hart, Phys. Stat. Sol. 37, 753, (1970).
- 12. U. Bonse, M. Hart, Z. Physik 190, 455 (1966).
- 13. M. Hart, Sci. Progr. (Oxford) 56, 429 (1969).
- 14. U. Bonse, M. Hart, G. H. Schwuttke, Phys. Stat. Sol. 33, 361 (1969).
- 15. E. te Kaat, PhD thesis, University of Münster (1968).
- 16. U. Bonse, E. te Kaat, Z. Physik 214, 16 (1968)
- 17. R. D. Deslattes, Appl. Phys. Lett. 15, 386 (1969).
- 18. M. Hart, J. Phys. 1D, Ser. 2, 1405 (1968).
- 19. M. Hart, A. D. Milne, J. Phys. 2E, Ser. 2, 646 (1969).
- 20. U Bonse, M. Hart, Z. Physik 194, 1 (1966).
- 21. U. Bonse, M. Hart, Acta Cryst. A24, 240 (1968).
- 22. U. Bonse, X-ray Optics and Microanalysis (G. Möllenstedt, K. H. Gaukler, eds.), Springer-Verlag, New York (1969).

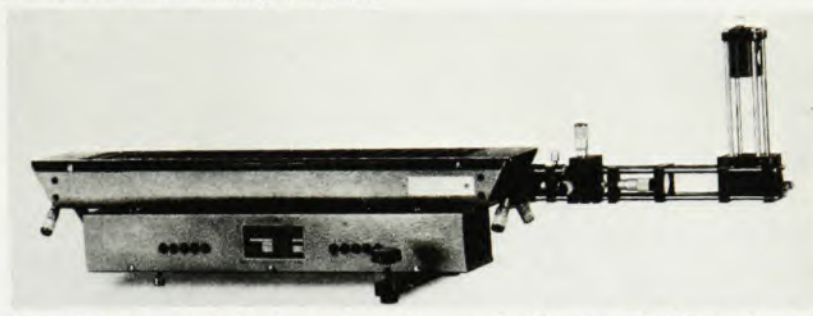
# PARTNERS IN RESEARCH

-for those who insist on time-and-money economy without sacrificing precision.





KLINGER announces the new Spindler and Hoyer partners in research—the HeNe 500N Laser, freshly and imaginatively redesigned in single unit construction to accommodate any desired components of the famous Micro Optical Bench.



In minutes, a micro optical system containing (among other things) a spatial filter, a beam expander, and a beam steerer has been coupled to the laser to make up a specialized instrument with precise automatic alignment and quickly available microadjustments.

The power supply for the 5.8 mw laser is built into the base; the resonators are dust-proof but readily accessible for dismantling; the mirror holders may be easily removed for mounting the laser and resonators on a standard optical bench. The ease with which the system may be switched from one application to another is unbelievable until you see it done or do it yourself.

We believe that this partnership will do more to minimize alignment problems, reduce develop-ment costs, increase flexibility, encourage experimental design changes, and improve prototype precision than anything you have ever used before.

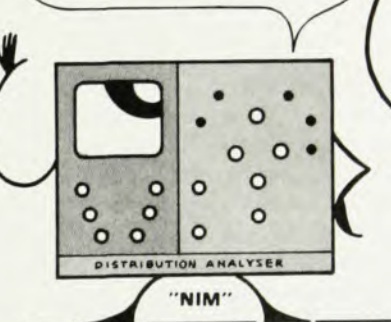
Price and all other details free upon request. Send for our Bulletin No. 500N. A postcard will do.

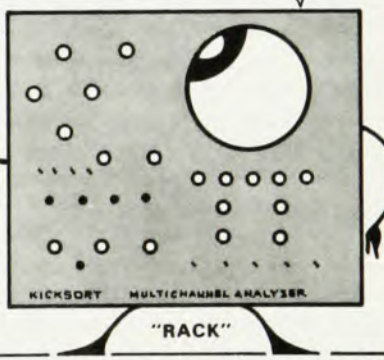
### KLINGER SCIENTIFIC APPARATUS CORP.

83-45 Parsons Blvd., Jamaica, New York 11432 (212) 657-0335

#### COMPATIBLES" "THE

WHY DO PHYSICISTS SCOFF AT MY SIMPLICITY, LACK OF COMPLEXITY, EASE OF OPERATION , AND SPEED WITH WHICH I DELIVER THE ANSWERS ? WHY DO STUDENTS AND ROUTINE ANALYSTS AVOID MY UNLIMITED FEATURES, SUCH AS: MULTISCALING, MÖSSBAUER , 60 MHZ 8192 ADC , AUTO PROGRAMMING, DIGITAL OFFSETS, LOG & LINEAR DISPLAY, EXPANDABLE MEMORY, SCA, ETC., ETC. ?





BECAUSE WE'RE BOTH NEEDED! (AND WE'RE BUDGET PRICED!)

Write in to find out exactly why everybody loves 2 & 400 channel "NIM" or 512, 1024 & 4096 channel "RACK" with all their NIM accessories.

e a u C r inc.

P.O. box 135, prairie view, illinois 60069 Telex 72-6407 Phone: 312-634-3870